

Searching for the elusive critical endpoint at finite isospin density and temperature

D. K. Sinclair (ANL)

J. B. Kogut (DOE and Maryland)

- Introduction
- Lattice QCD at finite isospin density.
- RHMC simulations of $N_f = 3$ lattice QCD at finite μ_I and T .
- RHMC for theories with unknown spectral bounds.
- Discussion and conclusions.

Introduction

We are interested in QCD at small quark-number chemical potential μ and temperature T . The most interesting feature of the QCD phase diagram in this regime is the critical endpoint.

QCD at finite isospin chemical potential μ_I has some similarities to QCD at finite μ , but lacks the sign problem. In particular, T_c for the finite-temperature transition at small μ_I appears to be the same as for small μ provided $\mu_I = 2\mu$. We conjecture that the critical endpoints might be coincident.

We are simulating 3-flavour lattice QCD (staggered fermions) at small μ_I and at T close to T_c on $8^3 \times 4$ and $12^3 \times 4$ lattices, for quark masses close to the

critical mass for zero chemical potentials. Fourth order Binder cumulants (B_4) are used to study the nature of the transition.

Because B_4 depends strongly on dt for the HMD(R) algorithm, we now use the exact RHMC algorithm for simulations.

Lattice QCD at finite isospin density

The staggered quark action for lattice QCD with N_f flavours at finite μ_I is

$$S_{pf} = p_\psi^\dagger \mathcal{M}^{-N_f/8} p_\psi \quad (1)$$

where p_ψ is the momentum conjugate to the pseudo-fermion field, and

$$\mathcal{M} = \left[\mathcal{D}(\frac{1}{2}\mu_I) + m \right]^\dagger \left[\mathcal{D}(\frac{1}{2}\mu_I) + m \right] + \lambda^2 \quad (2)$$

which is positive definite. For simulations at $\mu_I < m_\pi$, we set the symmetry-breaking parameter $\lambda = 0$.

The fourth-order Binder cumulant B_4 for an observable X is defined by

$$B_4(X) = \frac{\langle (X - \langle X \rangle)^4 \rangle}{\langle (X - \langle X \rangle)^2 \rangle^2} \quad (3)$$

$N_f = 3$ lattice QCD at finite μ_I and T

For $N_f = 3$ with quark masses $m < m_c$, the finite temperature transition at $\mu = \mu_I = 0$ is a first order phase transition. For $m > m_c$ this transition is a rapid crossover with no phase transition. At $m = m_c$ the transition is second order (critical point) in the 3-d Ising universality class.

As μ or μ_I is increased it has been argued that the critical mass would increase, becoming the critical endpoint. Hence, for m just above m_c one would expect to find a critical endpoint at small μ or μ_I . For this reason we are running $N_f = 3$ simulations for m close to m_c and small μ_I close to the finite temperature transition.

We are simulating lattice QCD with staggered fermions and $N_f = 3$ at quark masses close to m_c , on $12^3 \times 4$ and $8^3 \times 4$ lattices. We use $m = 0.02, 0.025, 0.03, 0.035$ and $\mu_I = 0.0, 0.2, 0.3$. For our $12^3 \times 4$ runs we perform runs of 300,000 trajectories at each of 4 β values close to the transition for each choice of m and μ_I . Most of these runs used $dt = 0.05$ which for length-1 trajectories gives RHMC acceptances of $\sim 70\%$.

On an infinite lattice the Binder cumulant for the chiral condensate, $B_4 = 3$ for a crossover, $B_4 = 1$ for a first order transition and $B_4 = 1.604(1)$ for a 3-d Ising critical point. β_c is obtained from minimum of B_4 obtained using Ferrenberg-Swendsen reweighting.

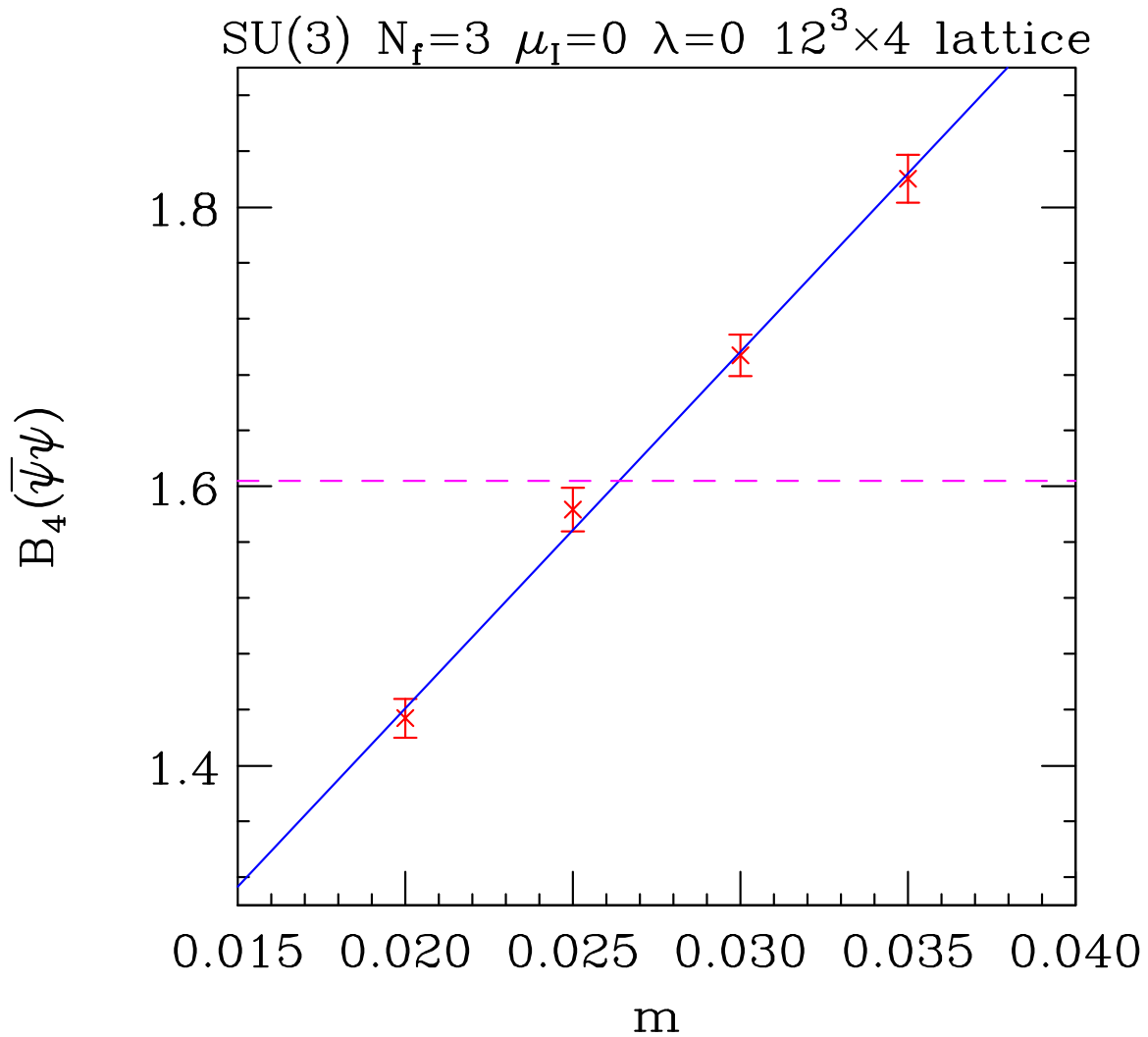


Figure 1: Binder cumulant at $T = T_c$ as a function of mass $\implies m_c = 0.0264(3)$.

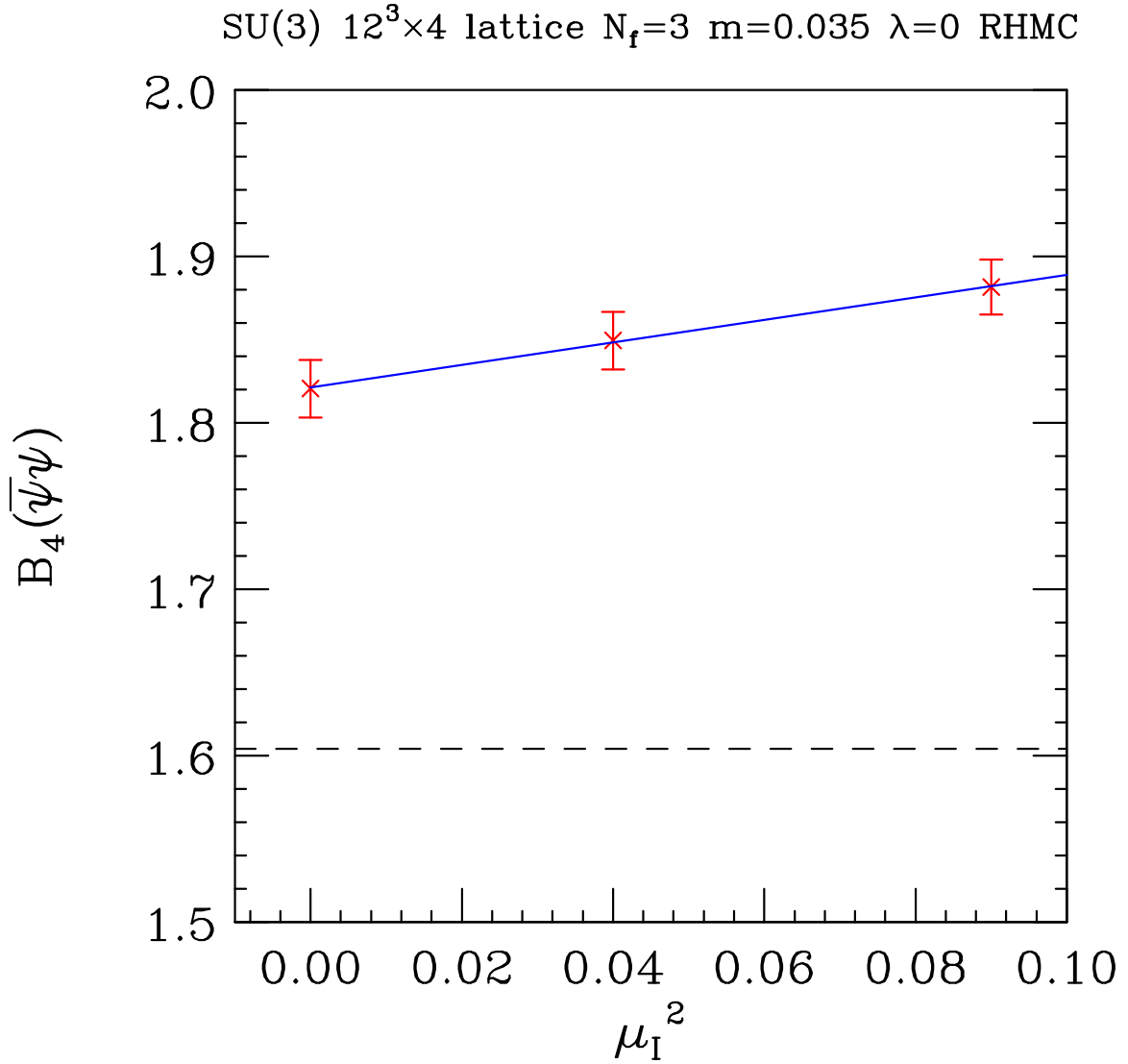


Figure 2: Binder cumulant at $T = T_c$ as a function of μ_I^2 at $m = 0.035$.

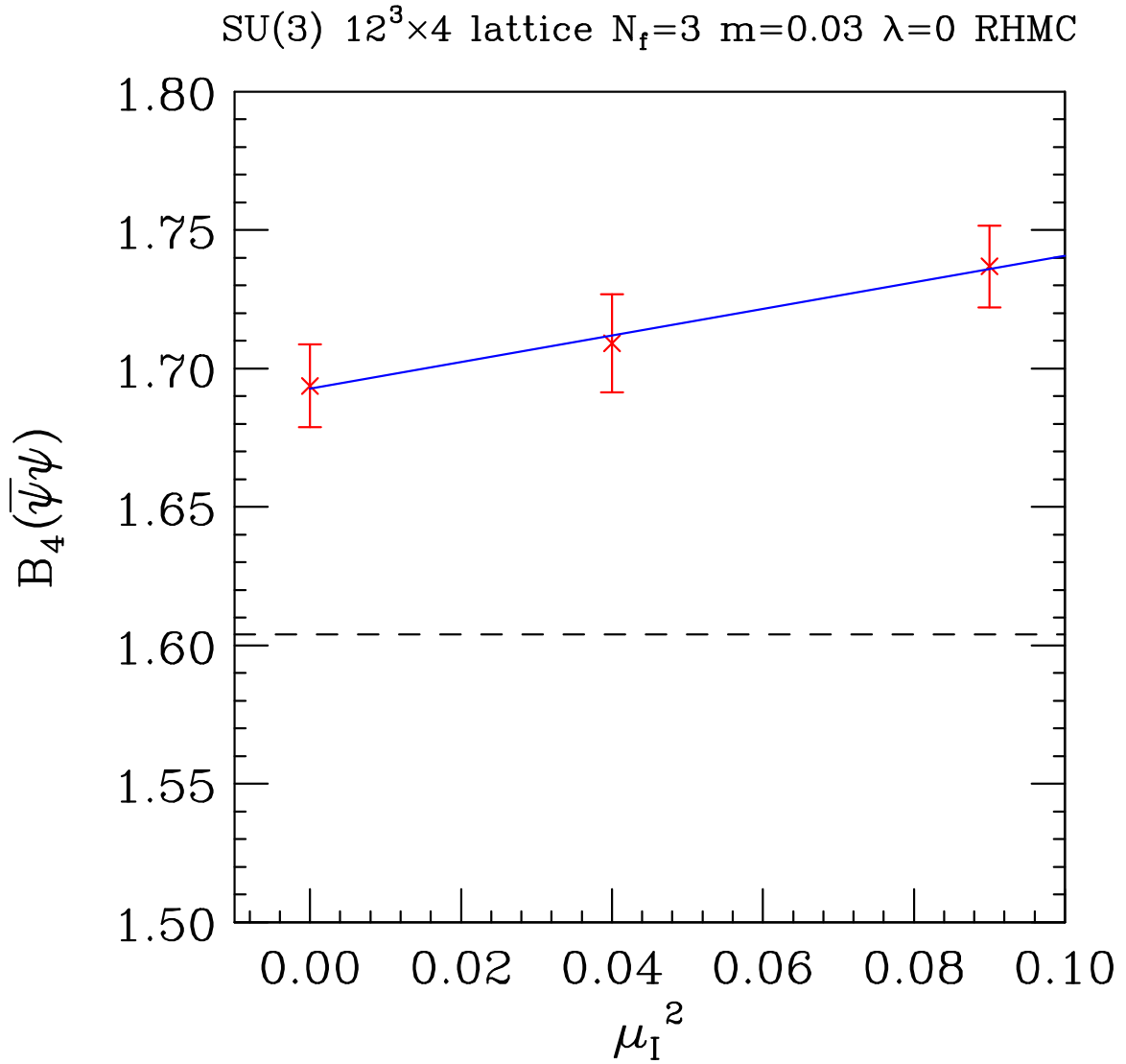


Figure 3: Binder cumulant at $T = T_c$ as a function of μ_I^2 at $m = 0.03$.

SU(3) $12^3 \times 4$ lattice $N_f=3$ $m=0.025$ $\lambda=0$ RHMC

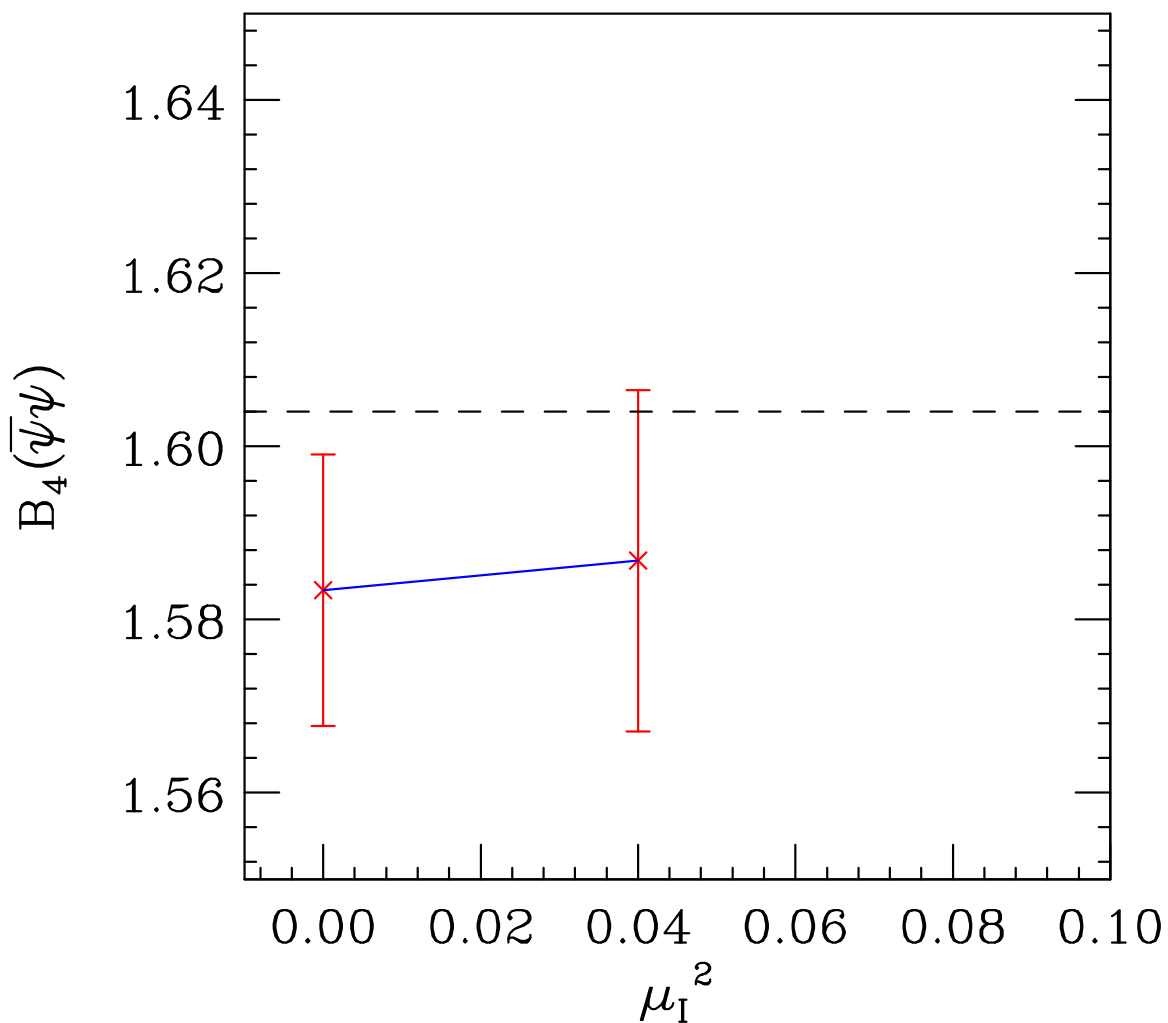


Figure 4: Binder cumulant at $T = T_c$ as a function of μ_I^2 at $m = 0.025$.

SU(3) $N_f=3$ $\lambda=0$, β s at minima of B_4

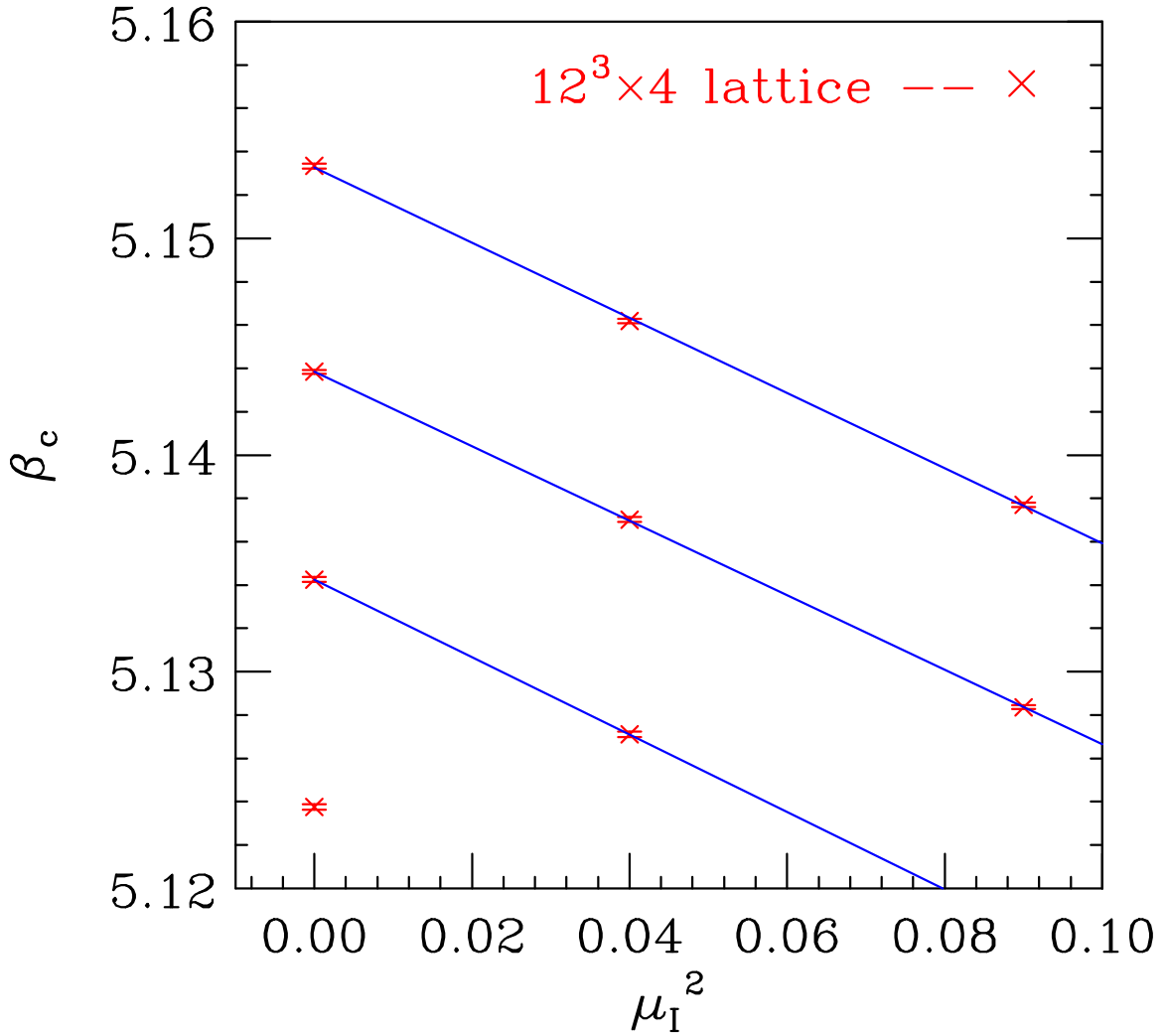


Figure 5: β_c at the transition from hadronic matter to a quark-gluon plasma as functions of μ_I^2 . From top to bottom, $m = 0.035$, $m = 0.03$, $m = 0.025$, $m=0.02$.

At $\mu_I = 0$, $m_c = 0.0264(3)$.

Binder cumulants show no sign of crossing the Ising value as μ_I is increased, for $m > m_c$. In fact they appear to increase slowly, rather than fall. Suggests critical endpoint is not connected with m_c .

To make the most of these relatively small lattices we should seek the scaling fields which are linear combinations of the chiral condensate, the gauge (plaquette) action and the isospin density. We should then seek the linear combination which minimizes the Binder cumulant, and examine its behaviour as a function of μ_I .

The straight line fits to $\beta_c(\mu_I)$ are:

$$\begin{aligned}
\beta_c &= 5.15326(10) - 0.173(2)\mu_I^2 & m &= 0.035 \\
\beta_c &= 5.14386(8) - 0.172(1)\mu_I^2 & m &= 0.030 \\
\beta_c &= 5.13426(12) - 0.179(4)\mu_I^2 & m &= 0.025
\end{aligned}
\tag{4}$$

The next figure shows the chiral susceptibilities at β_c obtained from their maxima using Ferrenberg-Swendsen reweighting.

$$\chi_{\bar{\psi}\psi} = V[\langle \bar{\psi}\psi^2 \rangle - \langle \bar{\psi}\psi \rangle^2] \tag{5}$$

where $\bar{\psi}\psi$ is a lattice averaged quantity normalized to 4 flavours, and V is the space-time volume. [Note that typically

$$\beta_c(B_4) - \beta_c(\chi_{\bar{\psi}\psi}) \sim 6 \times 10^{-5} \tag{6}$$

SU(3) $12^3 \times 4$ lattice $N_f=3$ $\lambda=0$ RHMC

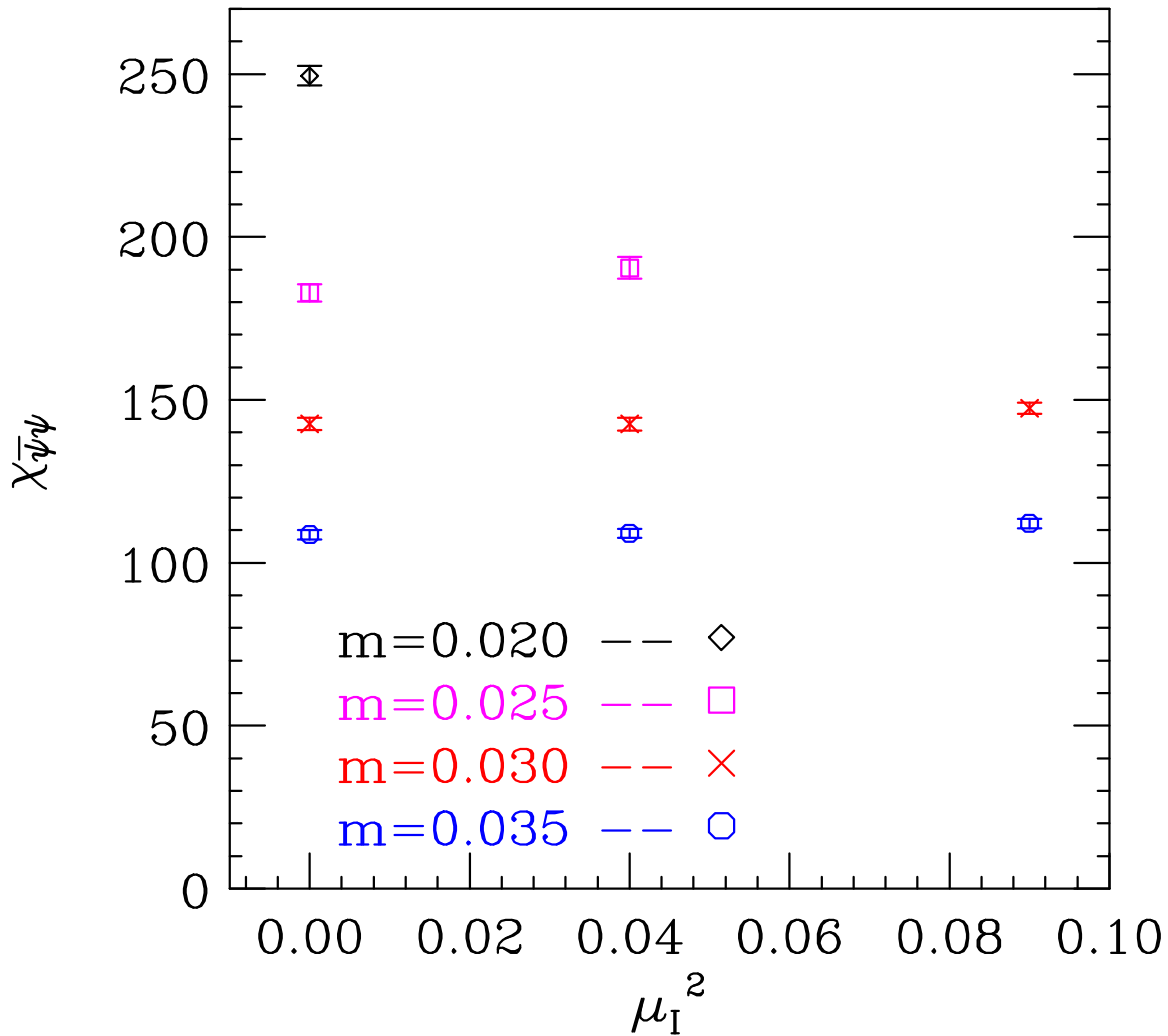


Figure 6: Chiral susceptibilities $\chi_{\bar{\psi}\psi}$ as functions of μ_I^2 for $m = 0.2, 0.25, 0.3, 0.35$. Note decrease with increasing m as transition softens.

RHMC for theories with unknown spectral bounds

QCD at finite μ_I

We know an upper bound on the spectrum of the quadratic Dirac operator to be

$$[\cosh(\frac{1}{2}\mu_I) + 3 + m]^2. \quad (7)$$

Choosing this value to be 25 more than covers the range of m and μ_I of interest.

Except at $\mu_I = 0$ we do not know a positive lower bound to this spectrum. At $\mu_I = 0$, knowing $m \geq 0.02$, a lower bound is 4×10^{-4} . For $\mu_I \geq 0$ we guess that 1×10^{-4} is a reasonable estimate for a lower bound over the range of μ_I s under consideration, and test this by

comparing measurements with extrapolations from HMD(R) results. In addition we compared our $\mu_I = 0.3$ results with those obtained using speculative lower bounds of 1×10^{-5} and 1×10^{-6} with the same parameter sets.

First we check reversibility of our implementation of the RHMC algorithm. This also checks that single (32 bit) precision floating-point arithmetic is adequate for the $12^3 \times 4$ lattices we use.

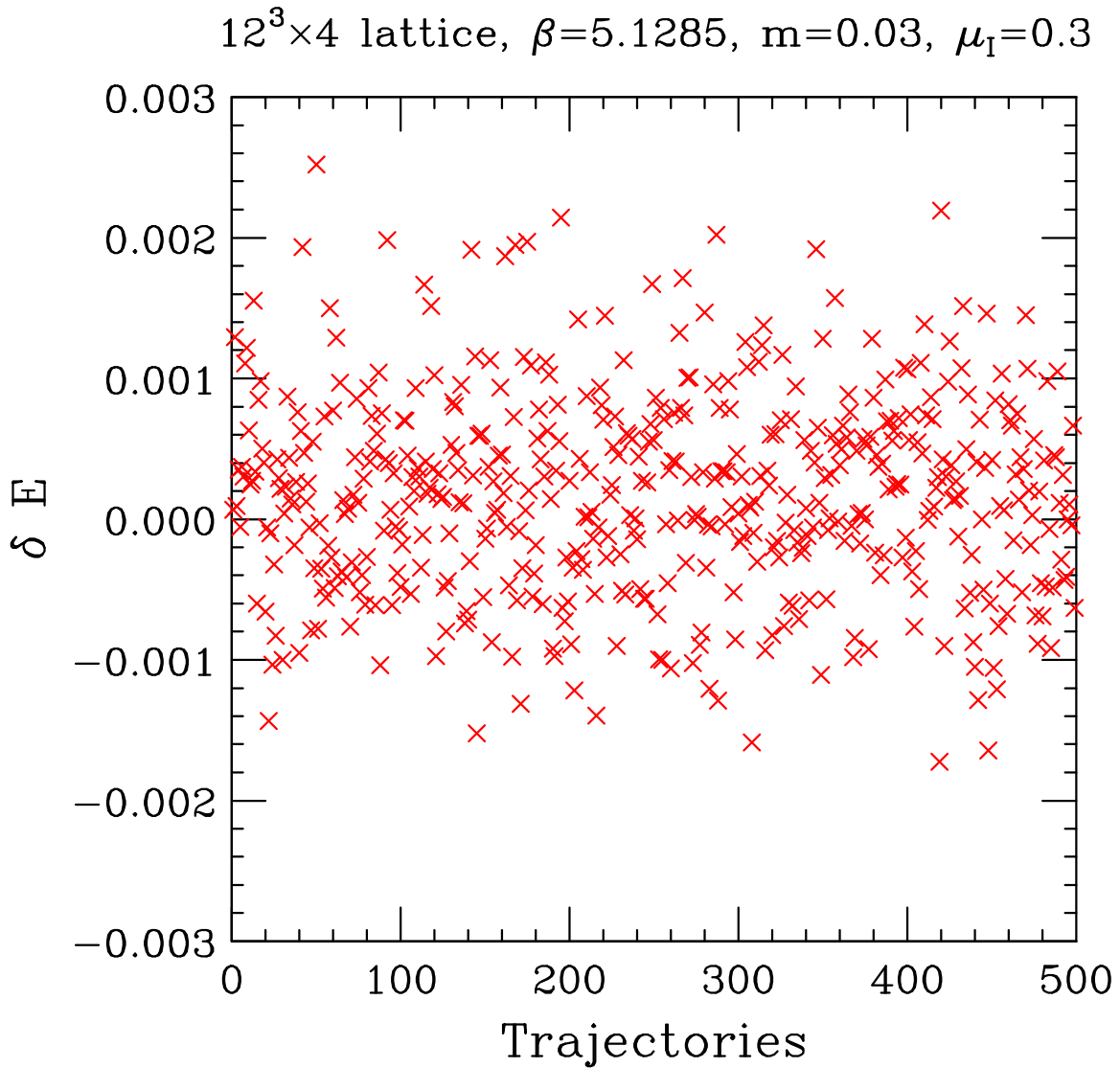


Figure 7: The ‘energy’ change for ‘closed’ trajectories ($t \rightarrow t + 1 \rightarrow t$).

$12^3 \times 4$ lattice, $\beta=5.1285$, $m=0.03$, $\mu_1=0.3$

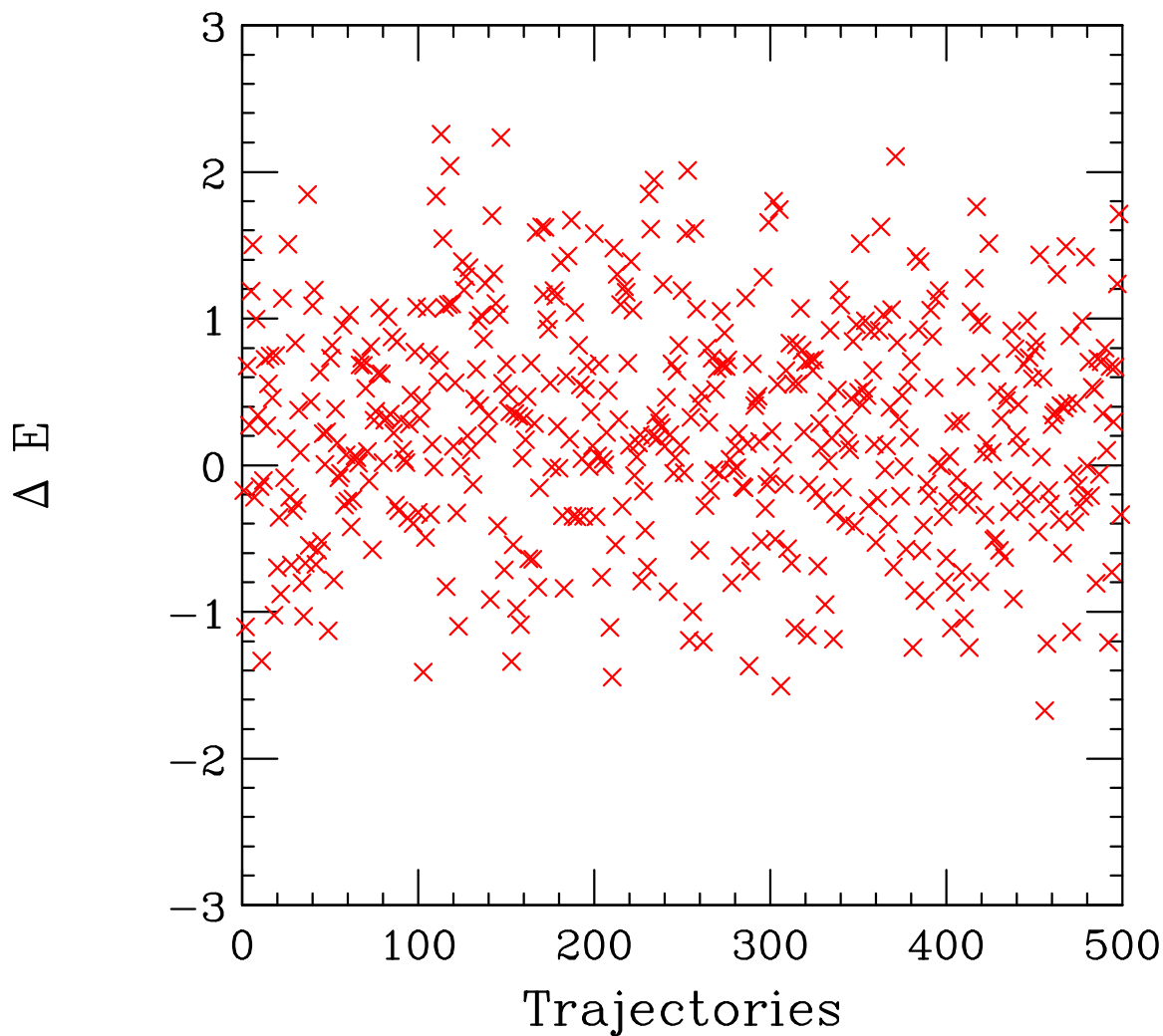


Figure 8: The ‘energy’ change for ‘open’ trajectories ($t \rightarrow t + 1$).

SU(3) $12^3 \times 4$ lattice $N_f=3$ $m=0.035$ $\mu_I=0.2$ $\lambda=0$

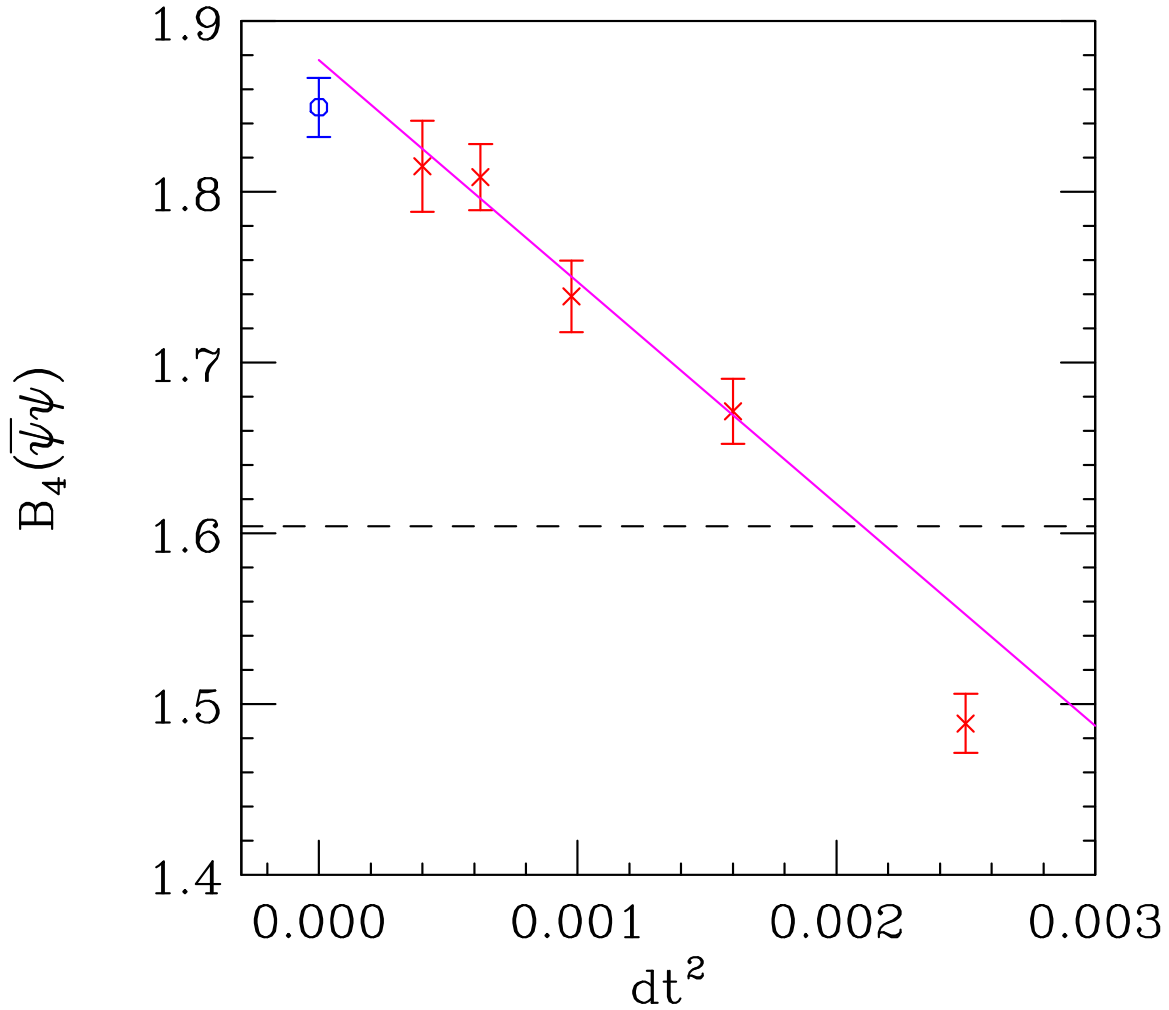


Figure 9: Binder cumulants for $m = 0.035$, $\mu_I = 0.2$ for HMD(R) simulations as a function of dt^2 compared with that from RHMC simulations.

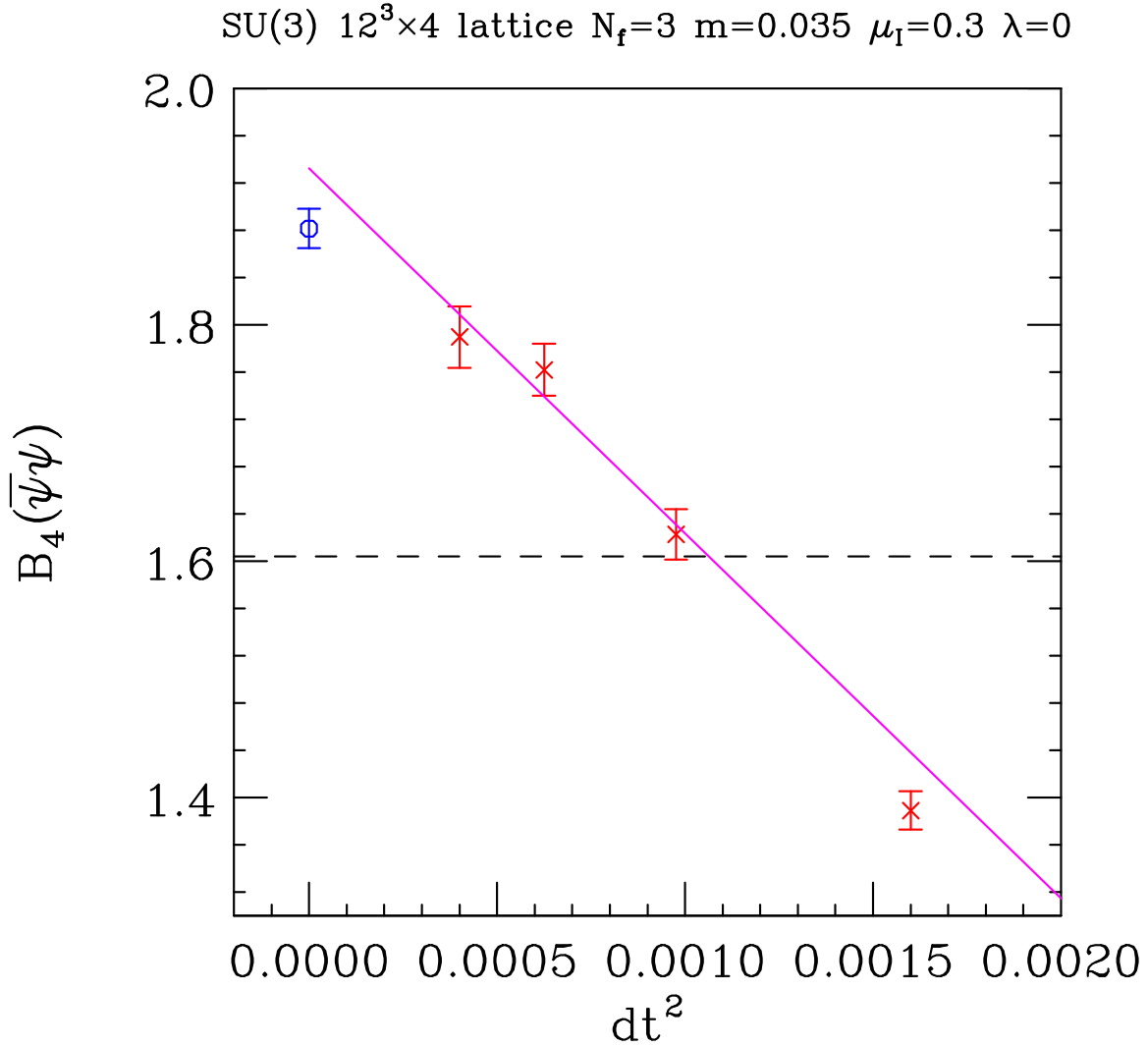


Figure 10: Binder cumulants for $m = 0.035$, $\mu_I = 0.3$ for HMD(R) simulations as a function of dt^2 compared with that from RHMC simulations.

SU(3) $12^3 \times 4$ lattice $N_f=3$ $m=0.035$ $\mu_I=0$ $\lambda=0$

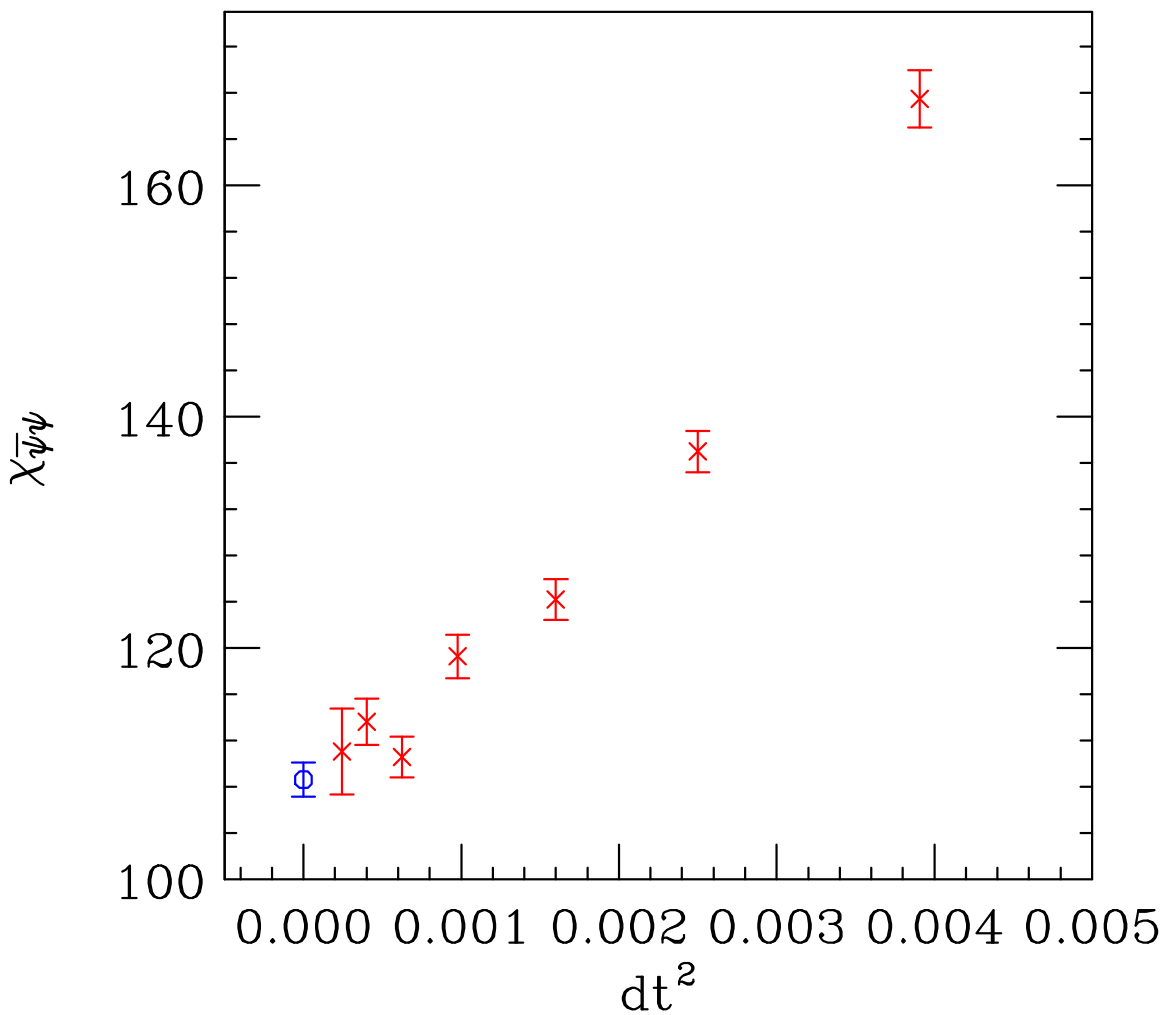


Figure 11: Chiral susceptibilities for $m = 0.035$, $\mu_I = 0$ for HMD(R) simulations as a function of dt^2 compared with that from RHMC simulations.

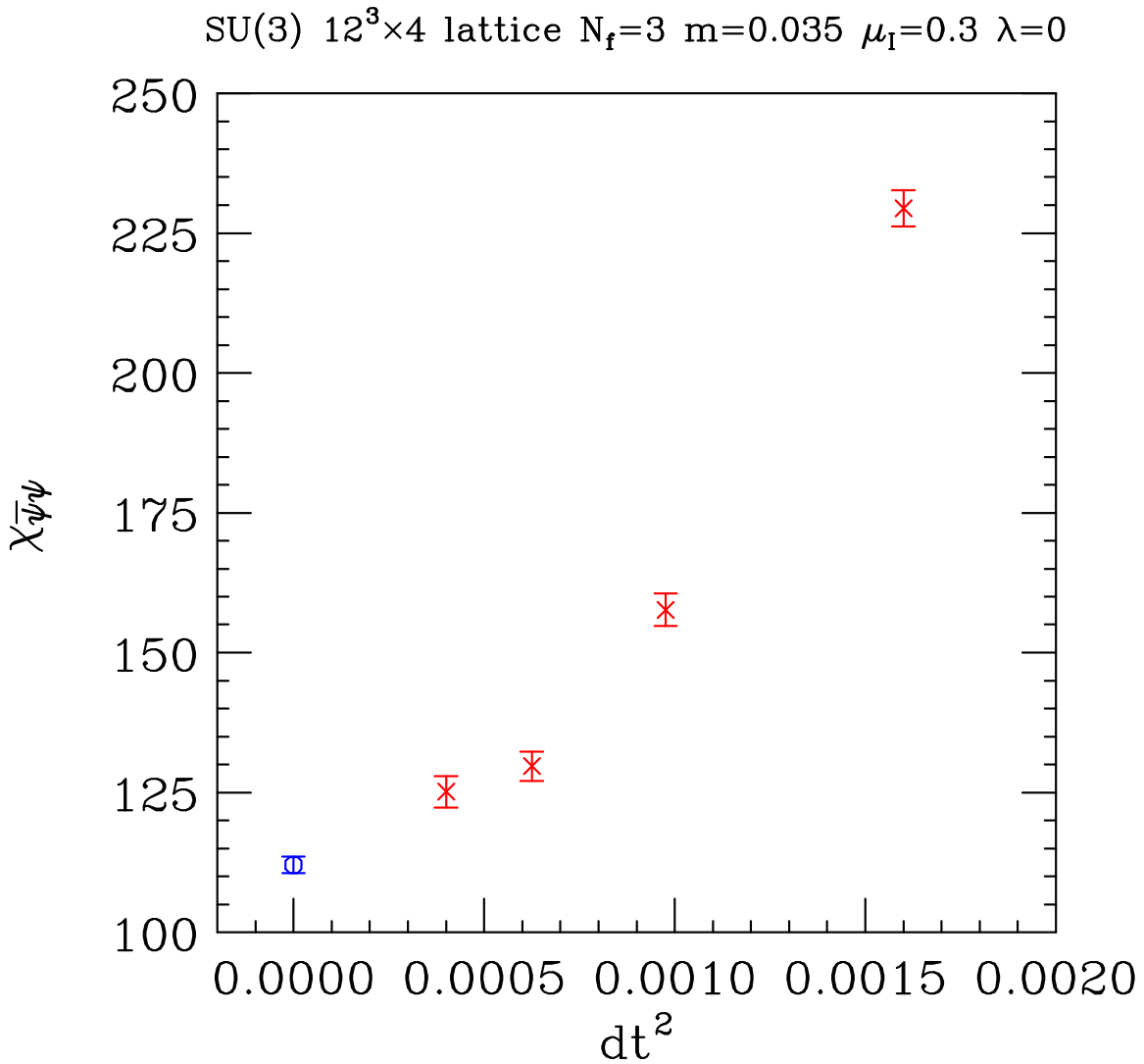


Figure 12: Chiral susceptibilities for $m = 0.035$, $\mu_I = 0.3$ for HMD(R) simulations as a function of dt^2 compared with that from RHMC simulations.

$m = 0.035, \mu_I = 0.3, \beta = 5.1370$		
Spectrum range	$[1 \times 10^{-4}, 25]$	$[1 \times 10^{-5}, 25]$
B_4	1.860(36)	1.879(41)
β_c	5.13744(24)	5.13787(22)
plaquette	0.51086(66)	0.51134(60)
Wilson Line	0.3300(74)	0.3245(68)
$\langle \bar{\psi}\psi \rangle$	0.6274(94)	0.6347(86)
j_0^3	0.0450(10)	0.0442(10)

$m = 0.03, \mu_I = 0.3, \beta = 5.1290$		
Spectrum range	$[1 \times 10^{-4}, 25]$	$[1 \times 10^{-6}, 25]$
B_4	1.704(30)	1.722(39)
β_c	5.12826(18)	5.12820(21)
plaquette	0.50776(60)	0.50753(68)
Wilson Line	0.3773(68)	0.3792(76)
$\langle \bar{\psi}\psi \rangle$	0.5442(80)	0.5411(103)
j_0^3	0.0529(10)	0.0532(11)

Table 1: Comparison of observables measured during RHMC simulations with different speculative lower bounds for the spectrum of the quadratic Dirac operator:

- a) For $m = 0.035, \mu_I = 0.3, \beta = 5.1370$.
- b) For $m = 0.030, \mu_I = 0.3, \beta = 5.1290$.

χ QCD

χ QCD is lattice QCD with irrelevant chiral 4-fermion interactions which allow simulations at zero quark mass.

For χ QCD, both upper and lower bounds of the spectrum of the quadratic Dirac operator are unknown. We are able to argue that 25 appears to be a ‘safe’ estimate for the upper bound. We know that very small eigenvalues do occur, although relatively infrequently. Our speculative lower bound which we check numerically is 10^{-6} .

Tests of reversibility indicate that on the relatively large lattices we use ($24^3 \times 8$), single precision (32-bit) floating point arithmetic is marginal, and double precision (64-bit) is preferred. We

have examined the effects of convergence criteria, both for initializing and ending trajectories, and for updating, on reversibility (and acceptance). Although convergence criteria can be less stringent for updating their effects on reversibility are at least as important as their effects on acceptance. This is due in part to stability issues and in part to differences in numbers of iterations of the multimass inverter for forward and reversed trajectories.

To check our speculative lower bound, we have compared rational approximations assuming a lower bound of 10^{-6} with those using a lower bound of 10^{-8} , at the beginning and at the end of each trajectory.

χ QCD $24^3 \times 8$ lattice, $\beta=5.535$, $\gamma=10$

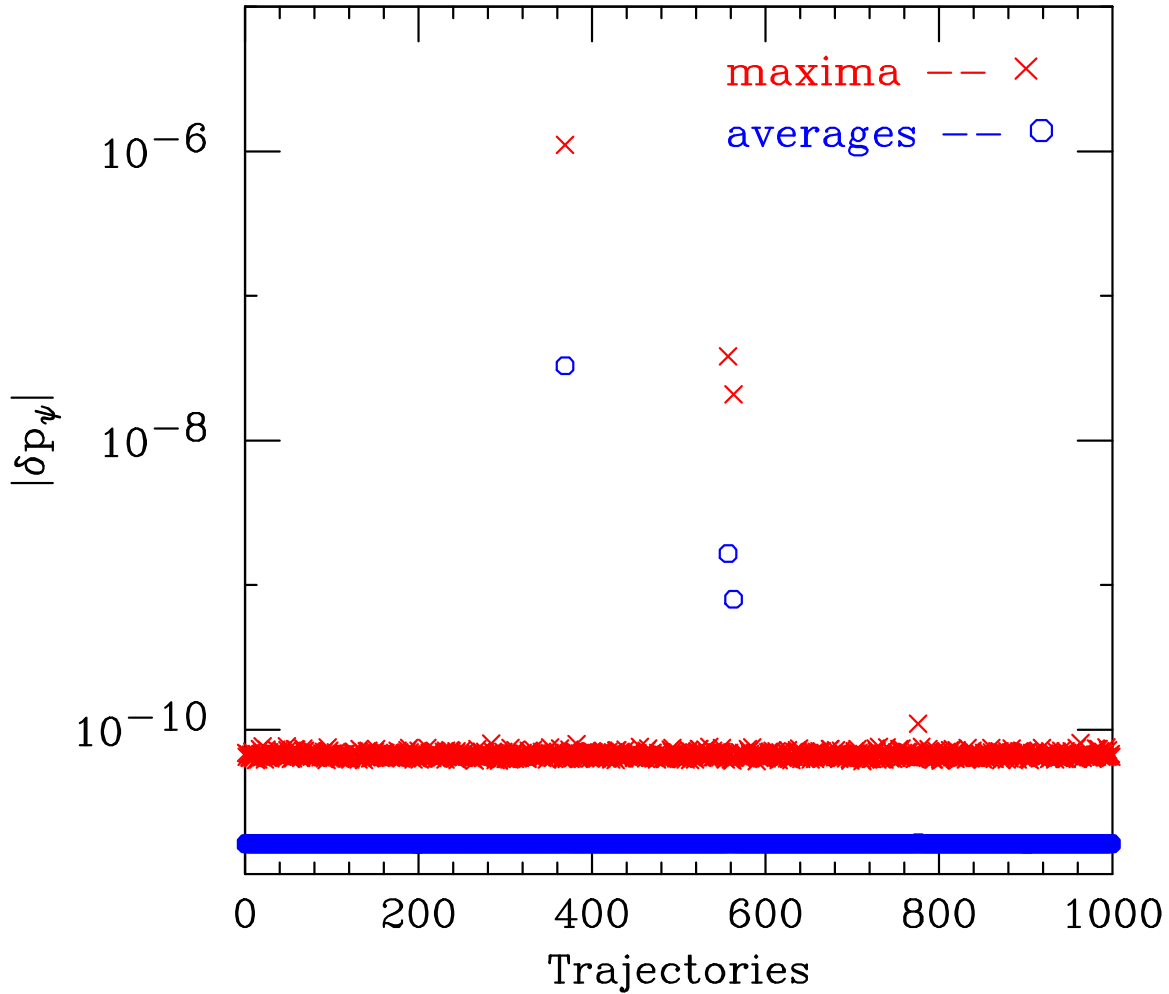


Figure 13: Difference in p_ψ values calculated assuming a lower spectral bound of 10^{-6} and those assuming a lower bound of 10^{-8} .

χ QCD $24^3 \times 8$ lattice, $\beta=5.535$, $\gamma=10$

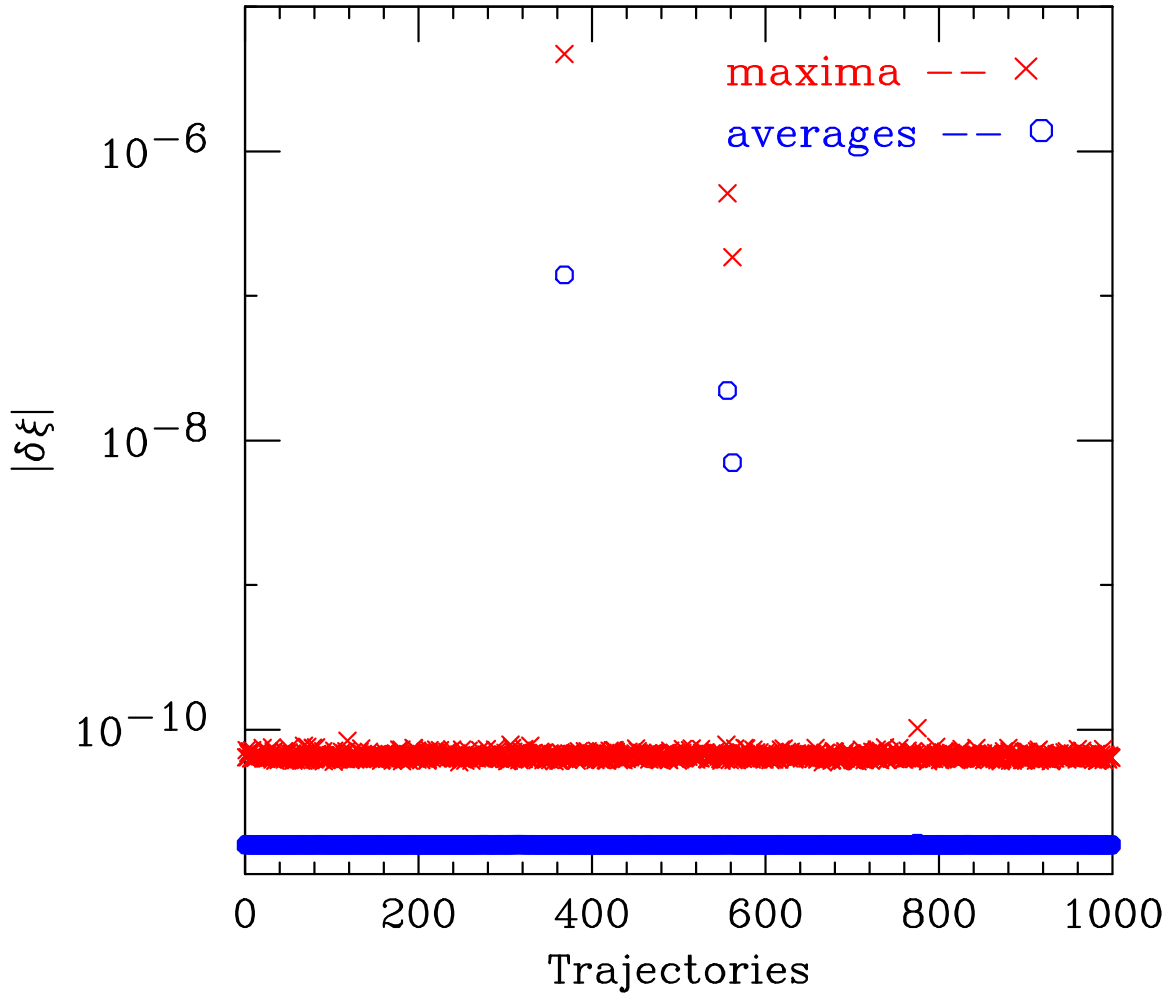


Figure 14: Difference in ξ values calculated assuming a lower spectral bound of 10^{-6} and those assuming a lower bound of 10^{-8} .

Discussion and conclusions

- We use 3-flavour simulations at finite μ_I to model behaviour at finite $\mu = \frac{1}{2}\mu_I$ (i.e. ignore phase of fermion determinant), close to the finite temperature transition.
- Because Binder cumulants used to determine nature of the finite temperature transition at finite μ_I depend strongly on dt in the HMD(R) scheme, we now use the RHMC algorithm.
- We see no sign of a critical endpoint over the range of μ_I considered (for $m > m_c$). Binder cumulant appears to rise with increasing μ_I .

- $12^3 \times 4$ simulations nearly finished. Complete $8^3 \times 4$ simulations. Binder cumulant analysis using scaling fields and/or use of larger lattices is needed. Improved actions?
- Our observations appear to agree with those at finite μ obtained using continuation from imaginary μ (by de Forcrand and Philipsen).
- With care, RHMC can be used, even where the lower bound on the spectrum of the quadratic Dirac operator is unknown. For QCD at finite μ_I and χ QCD there is no even-odd lattice separation. Having pseudo-fermions defined over whole lattice increases acceptance (Multiple pseudo-

fermions).

- Equation-of-state calculations should be performed with this theory.
- Simulations are performed on Jazz at Argonne, Tungsten and Cobalt at NCSA, Bassi and Jacquard at NERSC, DataStar at SDSC and PC's in Argonne HEP.